

# Hadronic transitions in bottomonia at Belle

Simon Eidelman<sup>1,2,3,\*</sup>  
for the Belle Collaboration

<sup>1</sup>Budker Institute of Nuclear Physics SB RAS, Novosibirsk, Russia

<sup>2</sup>Novosibirsk State University, Novosibirsk, Russia

<sup>3</sup>Lebedev Physical Institute RAS, Moscow, Russia

**Abstract.** Recent Belle results on various hadronic transitions among bottomonia are presented. We observe transitions with the  $\eta$  and  $\eta'$  meson at the  $\Upsilon(4S)$ . Bottomonium production together with the  $\eta$  meson is also reported at the  $\Upsilon(10860)$ . We study  $\pi^+\pi^-\pi^0$  transitions at the  $\Upsilon(10860)$  and  $\Upsilon(11020)$ .

## 1 Introduction

Spectroscopy of heavy quarkonia provides crucial information for understanding strong interactions since QCD calculations become possible. Measurements of hadronic transitions ( $\pi^+\pi^-$ ,  $\eta$ ,  $\omega$ , ...) between bottomonia yield important input for QCD.  $\eta$  transitions are believed to be suppressed compared to  $\pi^+\pi^-$  because of the spin flip.  $\pi^+\pi^-$  transitions and their peculiarities were studied by both BaBar and Belle. Large integrated luminosity collected by Belle above the  $\Upsilon(4S)$  opened unique possibilities resulting in exciting observations of  $h_b(1P)$ ,  $h_b(2P)$ ,  $\eta_b(2S)$ ,  $Z_b(10610)$  and  $Z_b(10650)$ . In this work we discuss recent results on hadronic transitions in bottomonia.

## 2 Study of $\eta$ and $\pi^+\pi^-$ transitions in $\Upsilon(4S)$ decays to lower $b\bar{b}$

Here we study the transitions  $\Upsilon(4S) \rightarrow \pi^+\pi^-\Upsilon(nS)$  ( $n = 1, 2$ ) and  $\Upsilon(4S) \rightarrow \eta\Upsilon(1S)$ , by reconstructing  $\Upsilon(nS) \rightarrow \mu^+\mu^-$ ,  $\eta \rightarrow \pi^+\pi^-\pi^0$  using  $(538 \pm 7) \times 10^6$   $\Upsilon(4S)$  mesons [1].

For the dipion transitions, the two-dimensional distribution of the invariant dimuon mass  $M(\mu\mu)$  vs.  $\Delta M$  for the selected events is shown in Fig. 1, where  $\Delta M = M(\pi\pi\mu\mu) - M(\mu\mu)$ . The signal yields are determined from the fit to the  $\Delta M$  distribution in  $6 \times 4$  ( $4 \times 4$ ) bins of  $M(\pi^+\pi^-)$  and  $\cos\theta_{\text{hel}}(\pi^+)$  in the regions (a) and (b) due to the initial-state radiation processes  $\Upsilon(2S) \rightarrow \pi^+\pi^-\Upsilon(1S)$  and  $\Upsilon(3S) \rightarrow \pi^+\pi^-\Upsilon(1S)$ , respectively (in (c) and (d) due to the decays of interest  $\Upsilon(4S) \rightarrow \pi^+\pi^-\Upsilon(1S)$  and  $\Upsilon(4S) \rightarrow \pi^+\pi^-\Upsilon(2S)$ , respectively). The results are listed in Table 1 and the  $\Delta M$  distributions integrated over the bins are shown in Fig. 2.

For the  $\eta$  transitions, the distributions of  $\Delta M_\eta = M(\pi\pi\gamma\mu\mu) - M(\mu\mu) - M(\pi\pi\gamma\gamma)$  are shown in Fig. 3 for the  $\Upsilon(4S) \rightarrow \eta\Upsilon(1S)$  (left) and  $\Upsilon(1^3D_{1,2}) \rightarrow \eta\Upsilon(1S)$  (right).

All the results are compatible with the previous measurements with the slightly improved precision. We confirm the enhancement of the  $\Upsilon(4S) \rightarrow \Upsilon(1S)$  transition via the spin-flip exchange of the  $\eta$  meson with respect to the dipion one.

\*e-mail: [simon.eidelman@cern.ch](mailto:simon.eidelman@cern.ch)

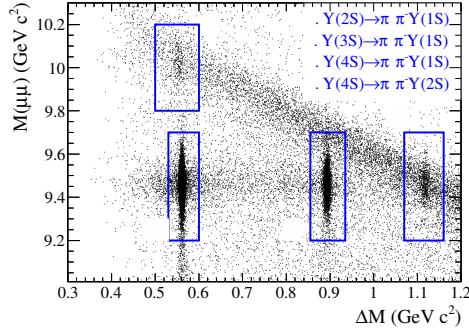


**Figure 1.** Distribution of  $M(\mu\mu)$  vs.  $\Delta M$  for the selected events. Fit regions are enclosed in boxes.

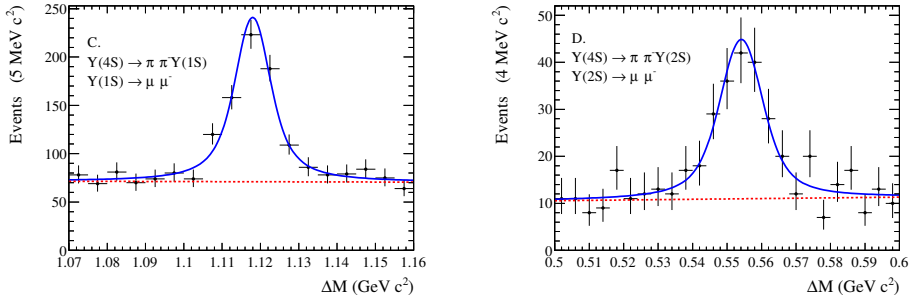


**Figure 2.** Fits to the  $\Delta M$  distributions for: (left)  $\Upsilon(4S) \rightarrow \pi^+\pi^-\Upsilon(1S)$  and (right)  $\Upsilon(4S) \rightarrow \pi^+\pi^-\Upsilon(2S)$ .

**Table 1.** The signal yields and branching fractions compared to PDG [2] for the decay modes studied.

Decay	Events	$\mathcal{B}, 10^{-5}$	$\mathcal{B}_{\text{PDG}}, 10^{-5}$
$\Upsilon(4S) \rightarrow \pi^+\pi^-\Upsilon(1S)$	$1095 \pm 74$	$8.2 \pm 0.5 \pm 0.4$	$8.1 \pm 0.6$
$\Upsilon(4S) \rightarrow \pi^+\pi^-\Upsilon(2S)$	$821 \pm 107$	$7.9 \pm 1.0 \pm 0.4$	$8.6 \pm 1.3$
$\Upsilon(4S) \rightarrow \eta\Upsilon(1S)$	$49 \pm 7$	$1.70 \pm 0.23 \pm 0.08$	$1.96 \pm 0.28$
$\Upsilon(1^3D_{1,2}) \rightarrow \eta\Upsilon(1S)$	$2.1 \pm 3.0$	$< 0.23$	–

### 3 Observation of $\Upsilon(4S) \rightarrow \eta'\Upsilon(1S)$

This observation is based on the same data sample of  $(538 \pm 7) \times 10^6$   $\Upsilon(4S)$  mesons as in Sect. 2. We reconstruct  $\Upsilon(1S) \rightarrow \mu^+\mu^-$  and  $\eta' \rightarrow \rho\gamma$ ,  $\eta\pi^+\pi^-$ ,  $\eta \rightarrow 2\gamma$  [3].

Signal events are identified by the variable  $\Delta M_{\eta'} = M(\Upsilon(4S)) - M(\Upsilon(1S)) - M(\eta')$ , where  $M(\Upsilon(1S)) = M(\mu\mu)$ ,  $M(\Upsilon(4S)) = M(\mu\mu\pi\pi\gamma)[M(\mu\mu\pi\pi\gamma\gamma)]$  and  $M(\eta') = M(\pi\pi\gamma)[M(\pi\pi\gamma\gamma)]$ . The signal and background yields are obtained by the fit to the  $\Delta M_{\eta'}$  distributions shown in Fig. 4 and are also listed in Table 2.

The combined branching fraction is  $\mathcal{B}(\Upsilon(4S) \rightarrow \eta'\Upsilon(1S)) = (3.43 \pm 0.88 \pm 0.21) \times 10^{-5}$  and corresponds to the  $5.7\sigma$  statistical significance.

We also determine the ratios of branching fractions:

$$R_{\eta'/h} = \frac{\mathcal{B}(\Upsilon(4S) \rightarrow \eta'\Upsilon(1S))}{\mathcal{B}(\Upsilon(4S) \rightarrow h\Upsilon(1S))}$$

**Table 2.** The signal and background yields as well as significances for two  $\eta'$  decay modes.

$\eta'$ decay mode	$N_{\text{sig}}$	$N_{\text{bkg}}$	Sign., $\sigma$
$2\pi 1\gamma$	$22 \pm 7$	$96 \pm 11$	4.2
$2\pi 2\gamma$	$5.0 \pm 2.3$	$2.0 \pm 1.6$	4.1

where the decay is mediated by  $h = \eta$  or  $h = \pi^+\pi^-$  and using the values from our work [1] obtain  $R_{\eta'/\eta} = 0.20 \pm 0.06$  and  $R_{\eta'/\pi^+\pi^-} = 0.42 \pm 0.11$ . The former ratio agrees with the predicted 0.2 [4].

#### 4 Observation of $\Upsilon(4S) \rightarrow \eta h_b(1P)$

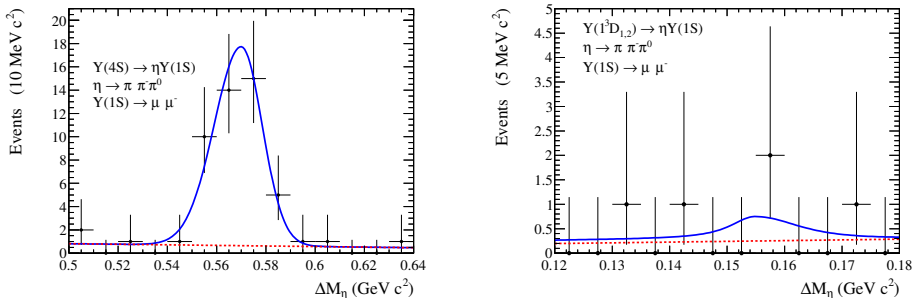
From a sample of  $771.6 \times 10^6$   $\Upsilon(4S)$  decays ( $711 \text{ fb}^{-1}$ ) Belle observed for the first time the decay  $\Upsilon(4S) \rightarrow \eta h_b(1P)$  using the  $\eta$  missing mass,  $M_{\text{miss}}(\eta) = \sqrt{(P_{e^+e^-} - P_\eta)^2}$  and  $\eta \rightarrow \gamma\gamma$  [5]. The  $M_{\text{miss}}(\eta)$  distribution is shown in Fig. 5 (left). The clear  $h_b(1P)$  signal is observed with the fit yield of  $112469 \pm 5537$  events ( $11\sigma$  significance).

The obtained branching fraction  $\mathcal{B}(\Upsilon(4S) \rightarrow \eta h_b(1P)) = (2.18 \pm 0.11 \pm 0.18) \times 10^{-3}$  agrees with the theoretical prediction of Ref. [6].

We reconstruct the  $h_b(1P) \rightarrow \gamma \eta_b(1S)$  decay by measuring the number of events of  $\Upsilon(4S)$  decay as a function of the variable  $\Delta M_{\text{miss}} = M_{\text{miss}}(\eta\gamma) - M_{\text{miss}}(\eta)$ . Its distribution (Fig. 5 (right)) shows a clear excess at  $\Delta M_{\text{miss}} = M_{\eta_b(1S)} - M_{h_b(1P)}$ , with a yield of  $33116 \pm 4741$  events ( $9\sigma$  significance). The corresponding branching fraction  $\mathcal{B}(h_b(1P) \rightarrow \gamma \eta_b(1S)) = (56 \pm 8 \pm 4)\%$  agrees with predictions [7, 8]. The results are summarized in Table 3.

**Table 3.** Summary of the searches for  $\Upsilon(4S) \rightarrow \eta h_b(1P)$  and  $h_b(1P) \rightarrow \gamma \eta_b(1S)$ .

Observable	Value, MeV
$M_{h_b(1P)}$	$9899.3 \pm 0.4 \pm 1.0$
$M_{\eta_b(1S)}$	$9400.7 \pm 1.7 \pm 1.6$
$\Gamma_{\eta_b(1S)}$	$8_{-5}^{+6} \pm 5$
$\Delta M_{\text{HF}}(1P) = M_{\chi_{bj}}^{\text{sa}}(1P) - M_{h_b(1P)}$	$+0.6 \pm 0.4 \pm 1.0$
$\Delta M_{\text{HF}}(1S) = M_{\Upsilon(1S)} - M_{\eta_b(1S)}$	$59.6 \pm 1.7 \pm 1.6$

**Figure 3.** Fits to the  $\Delta M_\eta$  distributions for: (left)  $\Upsilon(4S) \rightarrow \eta \Upsilon(1S)$  and (right)  $\Upsilon(1^3D_{1,2}) \rightarrow \eta \Upsilon(1S)$ .

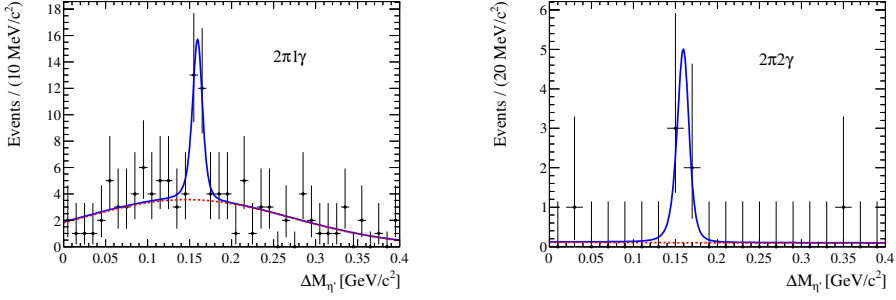


**Figure 4.** Fit to the  $\Delta M_\eta$  distribution for  $\Upsilon(4S) \rightarrow \eta'\Upsilon(1S)$  candidates in the  $2\pi 1\gamma$  (left) and  $2\pi 2\gamma$  (right) modes.

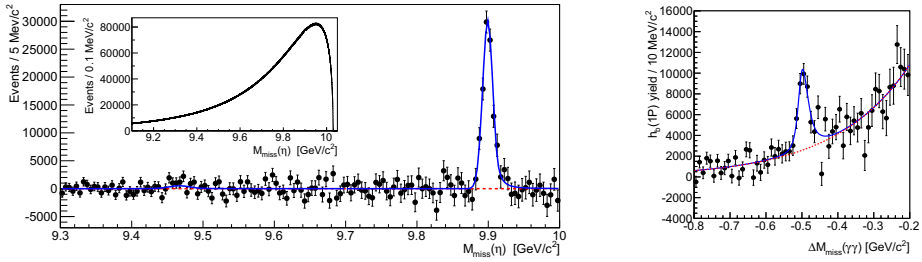


**Figure 5.** Distributions of: (left)  $M_{\text{miss}}(\eta)$  after background subtraction, (right)  $\Delta M_{\text{miss}}$ .

## 5 Production of $b\bar{b}$ and $\eta$ near $\Upsilon(5S)$

For this study we used a sample of  $121.4 \text{ fb}^{-1}$  collected near the  $\Upsilon(5S)$  energy [9]. The approach is based on the missing mass  $M_{\text{miss}}(\eta)$  similar to that in Sect. 4. The corresponding distribution is shown in Fig. 6 with the results listed in Table 4.

**Table 4.** Summary of the studies of  $e^+e^- \rightarrow \eta(b\bar{b})$  near  $\Upsilon(5S)$ .

Process	Sign., $\sigma$	$N, 10^3$	Process	Sign., $\sigma$	$N, 10^3$
$\eta\Upsilon(1S)$	$1.5\sigma$	$1.7 \pm 1.0$	$\eta\Upsilon(2S)$	$3.3\sigma$	$5.6 \pm 1.6$
$\eta h_b(1P)$	$2.7\sigma$	$3.9 \pm 1.5$	$\eta\Upsilon(1D)$	$5.3\sigma$	$9.3 \pm 1.8$

We observe for the first time the process  $e^+e^- \rightarrow \eta\Upsilon_J(1D)$  and find evidence for  $e^+e^- \rightarrow \eta\Upsilon(2S)$ . Assuming that the process proceeds entirely via the  $\Upsilon(5S)$  and taking  $\sigma(e^+e^- \rightarrow \Upsilon(5S)) = \sigma(e^+e^- \rightarrow b\bar{b}) = (0.340 \pm 0.016) \text{ nb}$  from our measurement [10], we obtain  $\mathcal{B}(\Upsilon(5S) \rightarrow \eta\Upsilon_J(1D)) = (4.82 \pm 0.92 \pm 0.67) \times 10^{-3}$ . This result agrees with theoretical estimates accounting for the effect of virtual  $B$ -meson loops [11]. We do not have significant evidence for  $e^+e^- \rightarrow \eta h_b(1P, 2P)$  nor  $e^+e^- \rightarrow \eta\Upsilon(1S)$ . We do not have direct evidence for the presence of the three states of the  $\Upsilon_J(1D)$  triplet and derive 90% CL upper limits on the fraction of  $J = 1$  and  $J = 3$  states with respect to the  $J = 2$  state.

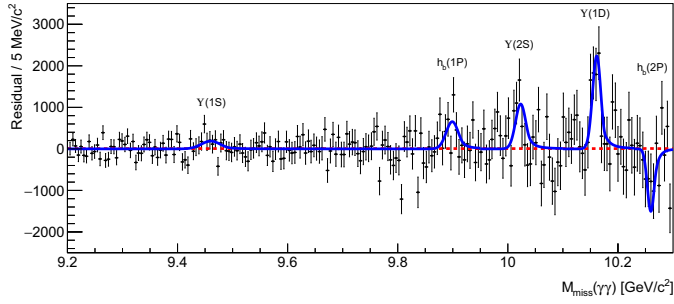


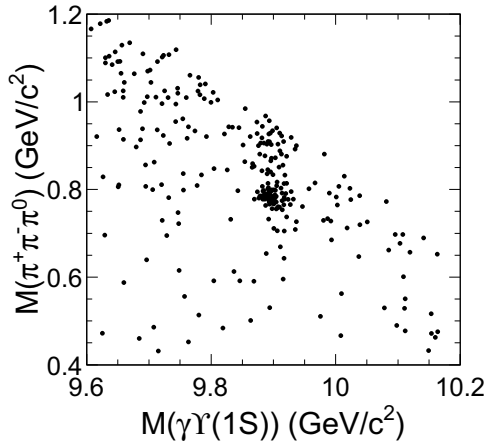
**Figure 6.**  $M_{\text{miss}}(\eta)$  distribution after subtraction of the fitted background.

## 6 Observation of $e^+e^- \rightarrow \pi^+\pi^-\pi^0\chi_{bJ}$ at 10.867 GeV

A data sample of  $118 \text{ fb}^{-1}$  collected at 10.867 GeV has been used to study  $\pi^+\pi^-\pi^0$  transitions between the  $\Upsilon(5S)$  and  $\chi_{bJ}$ ,  $J = 0, 1, 2$ , with subsequent  $\chi_{bJ} \rightarrow \gamma\Upsilon(1S)$ ,  $\Upsilon(1S) \rightarrow l^+l^-$ ,  $l = e, \mu$  decays [12].

Figure 7 shows the scatter plot of  $M(\pi^+\pi^-\pi^0)$  vs.  $M(\gamma\Upsilon(1S))$ . In addition to the clear  $\omega$  signal in the  $\chi_{bJ}$  mass region, there is an obvious accumulation of  $(\pi^+\pi^-\pi^0)_{\text{non-}\omega}$  events above the  $\omega$  mass. A two-dimensional fit gives the  $\omega\chi_{bJ}$  and  $(\pi^+\pi^-\pi^0)_{\text{non-}\omega\chi_{bJ}}$  yields. Figure 8 shows the  $\pi^+\pi^-\pi^0$  mass projection (left) with the obvious  $\omega$  signal and evidence for non- $\omega$  events, and the  $\gamma\Upsilon(1S)$  mass projection within (center) and outside (right) the  $\omega$  region with clear  $\chi_{b1}$  and  $\chi_{b2}$  signals. The fit results are summarized in Table 5. No excess of  $\chi_{b0}$  events above expected backgrounds is observed. The branching fractions of the three-pion transitions are large and of the same order as two-pion processes.

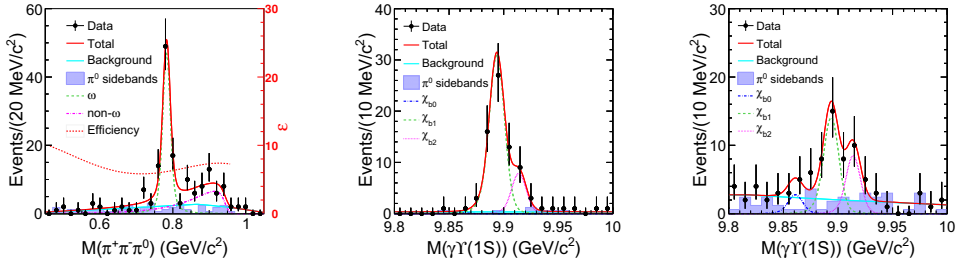
We also search for the  $X(3872)$ -like state  $X_b$  in the process  $e^+e^- \rightarrow \gamma X_b$ ,  $X_b \rightarrow \omega\Upsilon(1S)$  and observe no excess of events over the expectation from the  $\omega\chi_{bJ}$  final states. The upper limit is  $\mathcal{B}(\Upsilon(5S) \rightarrow \gamma X_b) \mathcal{B}(X_b \rightarrow \omega\Upsilon(1S)) < 2.9 \times 10^{-5}$  at 90% CL.



**Figure 7.** Scatter plot of  $M(\pi^+\pi^-\pi^0)$  vs.  $M(\gamma\Upsilon(1S))$  for selected  $e^+e^- \rightarrow \pi^+\pi^-\pi^0\gamma\Upsilon(1S)$  events.

**Table 5.** Results of the fits

Mode	Yield	Sign., ( $\sigma$ )	$\mathcal{B}$ , $10^{-3}$
$3\pi\chi_{b1}$	$80.1 \pm 9.9$	12	$1.85 \pm 0.23 \pm 0.23$
$3\pi\chi_{b2}$	$28.6 \pm 6.5$	5.9	$1.17 \pm 0.27 \pm 0.14$
$\omega\chi_{b1}$	$59.9 \pm 8.3$	12	$1.57 \pm 0.22 \pm 0.21$
$\omega\chi_{b2}$	$12.9 \pm 4.8$	3.5	$0.60 \pm 0.23 \pm 0.15$
$(3\pi)\text{non-}\omega\chi_{b1}$	$23.6 \pm 6.4$	4.9	$0.52 \pm 0.15 \pm 0.11$
$(3\pi)\text{non-}\omega\chi_{b2}$	$15.6 \pm 5.4$	3.1	$0.61 \pm 0.22 \pm 0.28$

**Figure 8.** Projections of: (left)  $M(\pi^+\pi^-\pi^0)$  for  $9.8 < M(\gamma Y(1S)) < 10$  GeV, (center)  $M(\gamma Y(1S))$  in the  $\omega$  region, (right)  $M(\gamma Y(1S))$  outside of the  $\omega$  region.

Finally, we search for  $Y(6S) \rightarrow \omega\chi_{bJ}, \phi\chi_{bJ}$  using scan data near 10.867 and 11.020 GeV [13]. We observe  $e^+e^- \rightarrow \pi^+\pi^-\pi^0\chi_{b1}$  near  $Y(6S)$  and find evidence for  $\omega\chi_{bJ}$  while there is no significant signals for  $\phi\chi_{bJ}$  from 10.96 to 11.05 GeV.

We thank the KEKB group for excellent operation of the accelerator. This work was supported by Ministry of Science and Higher Education of the Russian Federation, contract 14.W03.31.0026.

## References

- [1] E. Guido *et al.*, Phys. Rev. D **96**, 052005 (2017)
- [2] C. Patrignani *et al.*, Chin. Phys. C **40**, 100001 (2016)
- [3] E. Guido *et al.*, Phys. Rev. Lett. **121**, 062001 (2018)
- [4] M.B. Voloshin, Mod. Phys. Lett. A **26**, 773 (2011)
- [5] U. Tamponi *et al.*, Phys. Rev. Lett. **115**, 142001 (2015)
- [6] F.-K. Guo, C. Hanhart and U.-G. Meissner, Phys. Rev. Lett. **105**, 162001 (2010)
- [7] S. Godfrey and J.L. Rosner, Phys. Rev. D **66**, 014012 (2002)
- [8] D.-Y. Chen, X. Liu and T. Matsuki, Phys. Rev. D **87**, 094010 (2013)
- [9] U. Tamponi *et al.*, Eur. Phys. J. **78**, 633 (2018)
- [10] S. Esen *et al.*, Phys. Rev. D **87**, 031101 (2013)
- [11] B. Wang, D.Y. Chen and X. Liu, Phys. Rev. D **94**, 094039 (2016)
- [12] X.H. He *et al.*, Phys. Rev. Lett. **113**, 142001 (2014)
- [13] J.H. Yin *et al.*, arXiv:1806.06203